Cell Reports Medicine, Volume *4*

Supplemental information

CYP19A1 mediates severe SARS-CoV-2 disease outcome in males

Stephanie Stanelle-Bertram, Sebastian Beck, Nancy Kouassi Mounogou, Berfin Schaumburg, Fabian Stoll, Amirah Al Jawazneh, Zoé Schmal, Tian Bai, Martin Zickler, Georg Beythien, Kathrin Becker, Madeleine de la Roi, Fabian Heinrich, Claudia Schulz, Martina Sauter, Susanne Krasemann, Philine Lange, Axel Heinemann, Debby van Riel, Lonneke Leijten, Lisa Bauer, Thierry P.P. van den Bosch, Boaz Lopuhaä, Tobias Busche, Daniel Wibberg, Dirk Schaudien, Torsten Goldmann, Anna Lüttjohann, Jenny Ruschinski, Hanna Jania, Zacharias Müller, Vinicius Pinho dos Reis, Vanessa Krupp-Buzimkic, Martin Wolff, Chiara Fallerini, Margherita Baldassarri, Simone Furini, Katrina Norwood, Christopher Käufer, Nina Schützenmeister, Maren von Köckritz-Blickwede, Maria Schroeder, Dominik Jarczak, Axel Nierhaus, Tobias Welte, Stefan Kluge, Alice C. McHardy, Frank Sommer, Jörn Kalinowski, Susanne Krauss-Etschmann, Franziska Richter, Jan von der Thüsen, Wolfgang Baumgärtner, Karin Klingel, Benjamin Ondruschka, GEN-COVID Multicenter Study Group, Alessandra Renieri, and Gülsah Gabriel

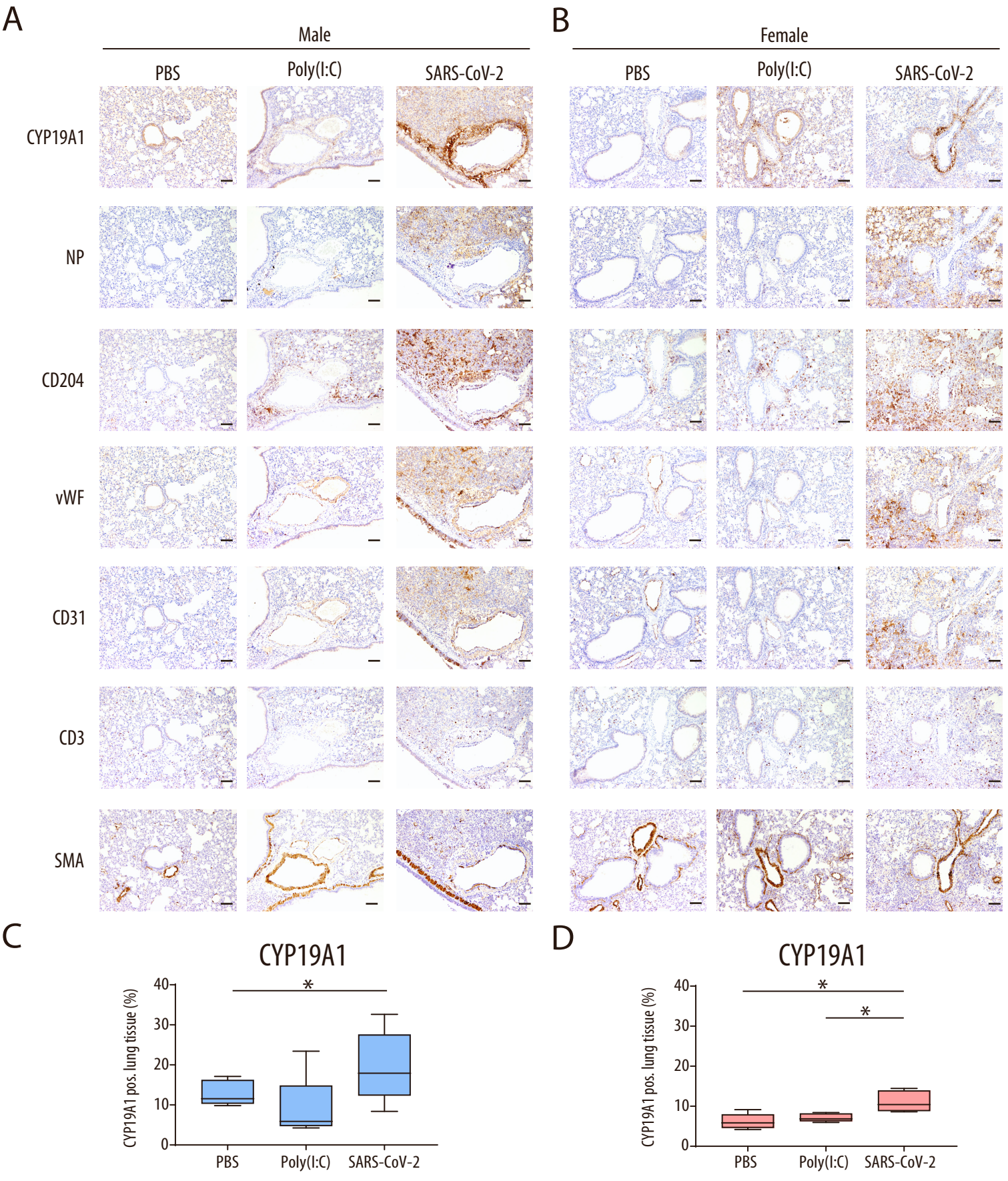

Figure S1. CYP19A1 protein expression in the lungs of SARS-CoV-2 infected male and female golden hamsters, Related to Figure 3.

(A, B) Immunohistochemistry of serial sections from the lungs of SARS-CoV-2 infected and control treated (PBS, Poly(I:C)) male (A) and female (B) golden hamsters for CYP19A1, SARS-CoV-2 NP, macrophages (CD204), endothelial cells (vWF and CD31), T cells (CD3) and smooth muscle actin (SMA). Representative pictures of each group are shown ($n = 5$). Scale bar, 100 µm. (C, D) Quantification of CYP19A1 expressing tissue in the lungs of SARS-CoV-2 infected and control treated (PBS, Poly(I:C)) male (C) and female (D) golden hamsters ($n = 5$). Data from PBS treated animals are also shown in Figure 3B. Data are shown as a box and whisker plot. Statistical significance was assessed by one-way ANOVA (*$p \leq 0.05$).

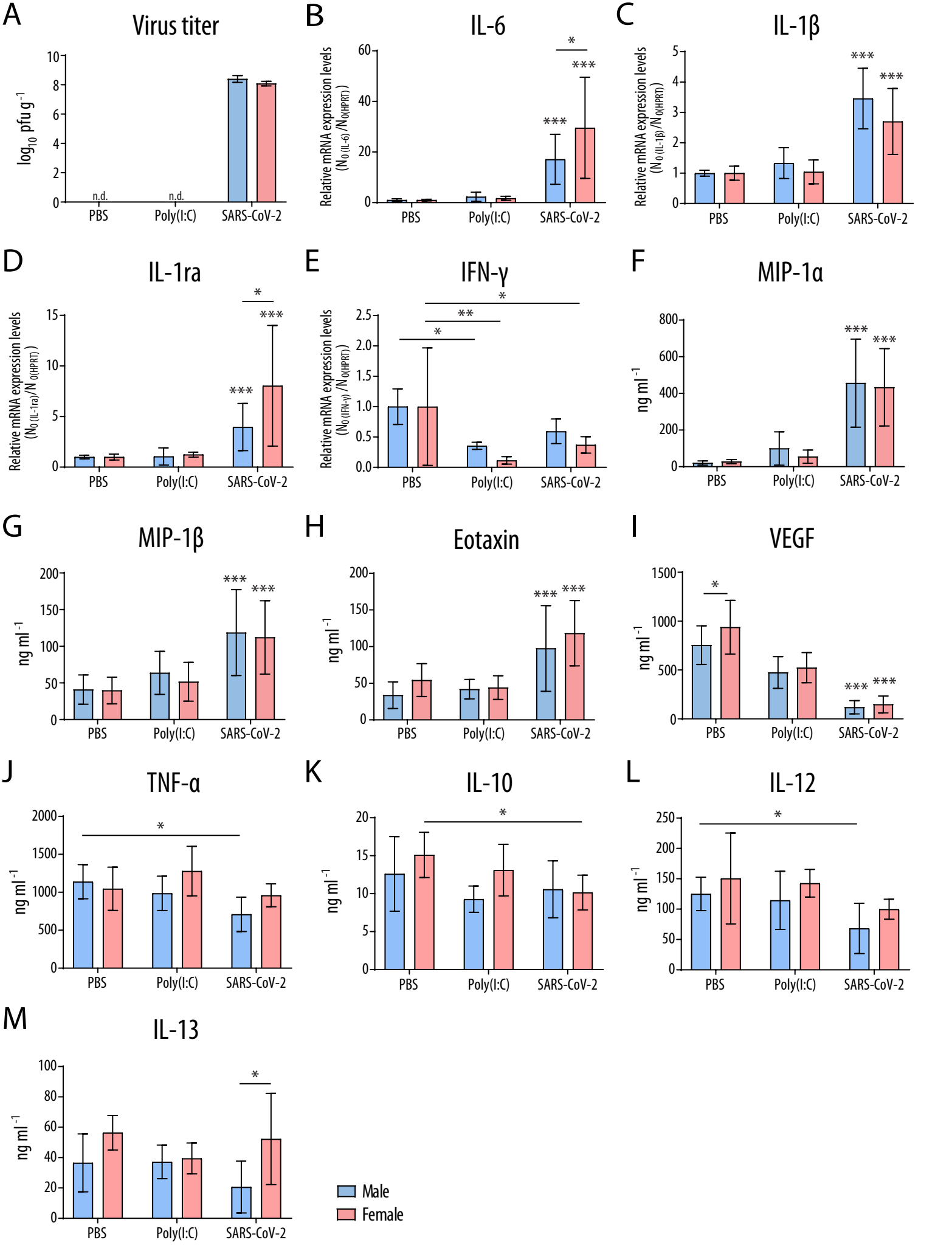
A
Virus titer
log10 pfu g-1
n.d.
n.d.
PBS
Poly(I:C)
SARS-CoV-2
B
IL-6
Relative mRNA expression levels (N0 (IL-6) /N0(HPRT))
C
IL-1β
Relative mRNA expression levels (N0 (IL-1β) /N0(HPRT))
D
IL-1ra
Relative mRNA expression levels (N0 (IL-1ra)/N0(HPRT))
E
IFN-γ
Relative mRNA expression levels (N0 (IFN-γ) /N0(HPRT))
F
MIP-1α
ng ml-1
G
MIP-1β
ng ml-1
H
Eotaxin
ng ml-1
I
VEGF
ng ml-1
J
TNF-α
ng ml-1
K
IL-10
ng ml-1
L
IL-12
ng ml-1
M
IL-13
ng ml-1
Male
Female

Figure S2. Virus replication and immune response in lungs of SARS-CoV-2 infected male and female golden hamsters, Related to Figure 3.

(A) Viral lung titers of infected male and female golden hamsters on day 3 p.i. (*n* = 5). Data of viral lung titers are also shown in Figure 4A, F, K and P. (B-E) IL-6 (B), IL-1β (C), IL-1 receptor antagonist (ra) (D) and IFN-γ (E) mRNA expression levels in SARS-CoV-2 infected male and female golden hamsters at day 3 p.i. (*n* = 5, male Poly(I:C): *n* = 4). Relative mRNA expression values in PBS treated hamsters were set to 1 after normalization against HPRT. (F-M) MIP-1α (*n* = 5) (F), MIP-1β (*n* = 5) (G), eotaxin (*n* = 5; male Poly(I:C): *n* = 4) (H), VEGF (*n* = 4; SARS-CoV-2: *n* = 3) (I), TNF-α (*n* = 5) (J), IL-10 (*n* = 5) (K), IL-12 (*n* = 5) (L) and IL-13 (*n* = 5) (M) protein expression levels in SARS-CoV-2 infected male and female golden hamsters at day 3 p.i.. Values are shown as means; error bars are shown as SD. Statistical significance was assessed by two-way ANOVA (*$p \leq 0.05$, **$p<0.01$, ***$p<0.001$).

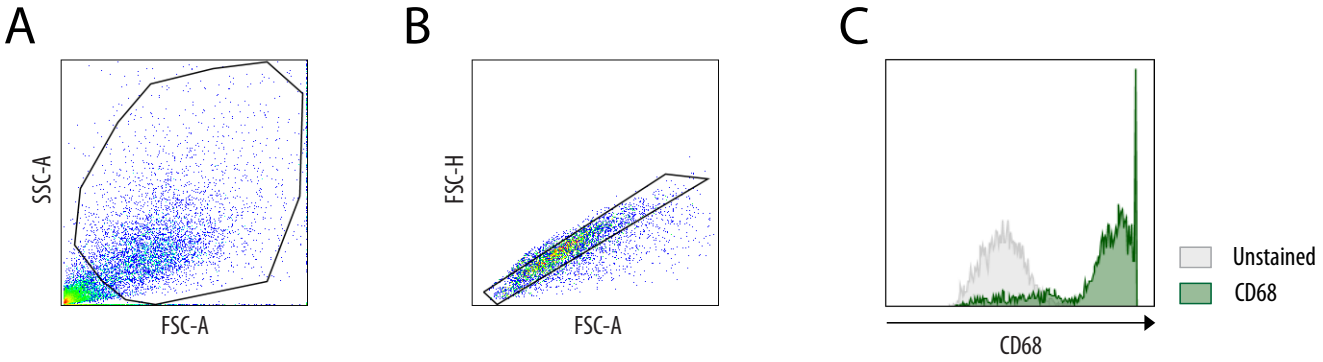

Figure S3. Characterization of ex vivo lung macrophages of golden hamsters, Related to Figure 3.

(A-C) Macrophages were isolated from the lung of a male hamster and their purity was assessed using fluorescence-activated cell sorting (FACS). Shown is the FACS gating strategy, including the removal of dead cells (A) and cell aggregates (B) via the use of forward and side scatter characteristics. Macrophages were stained using the macrophage marker protein CD68 (C).

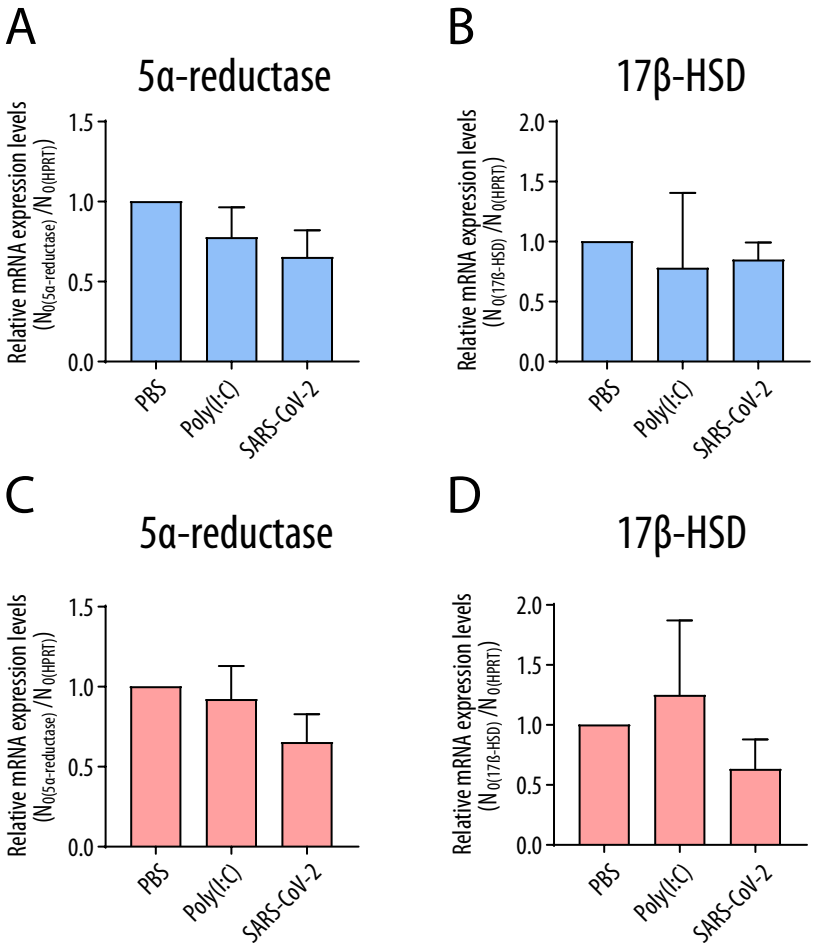

Figure S4. 5α-reductase and 17β-hydroxysteroid-dehydrogenase levels in the lungs of SARS-CoV-2 infected of male and female golden hamsters, Related to Figure 3.

(A, C) 5α-reductase mRNA expression levels measured in the lungs of SARS-CoV-2 infected and control treated (PBS, Poly(I:C)) male (A) and female (C) golden hamsters at day 3 p.i.. (B, D) 17β-hydroxysteroid-dehydrogenase (17β-HSD) mRNA expression levels measured in the lungs of SARS-CoV-2 infected and control treated (PBS, Poly(I:C)) male (B) and female (D) golden hamsters at day 3 p.i.. Relative mRNA expression values in PBS treated hamsters were set to 1 after normalization against HPRT. Values are shown as means; error bars are shown as SD (n = 5, male Poly(I:C): n = 4).

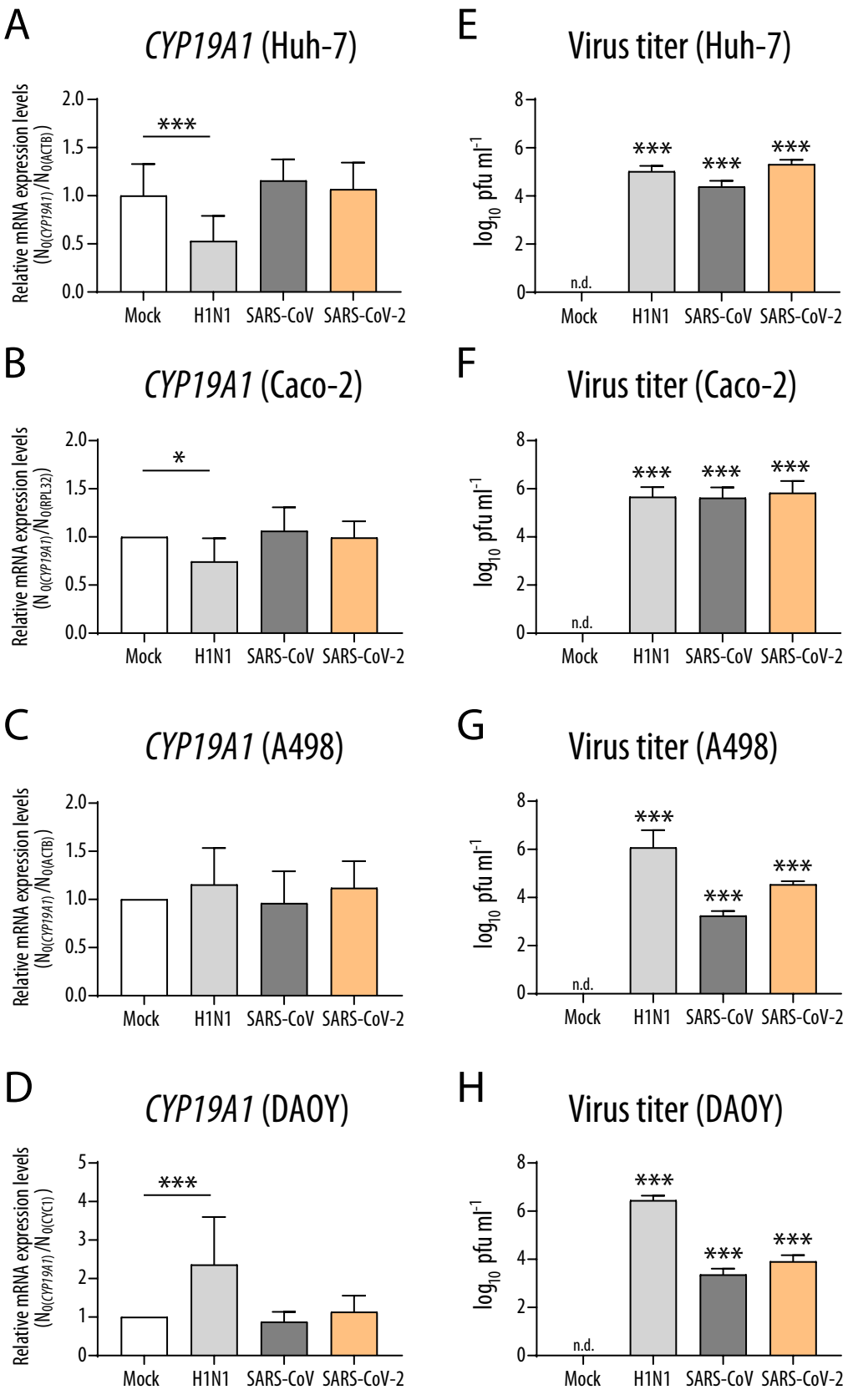

Figure S5. CYP19A1 mRNA expression in non-respiratory cell lines after respiratory virus infection, Related to Figure 3.

CYP19A1 mRNA expression levels (A-D) and virus titers (E-H) in Huh-7 (A, E), Caco-2 (B, F), A498 (C, G) and DAOY (D, H) cells control treated (Mock) or infected with H1N1 influenza A virus, SARS-CoV and SARS-CoV-2 (MOI 0.5) at 24 h p.i.. Shown is a merge of two to three independent biological replicates, each performed in technical triplicates. Relative CYP19A1 mRNA expression values in Mock treated cells were set to 1 after normalization against the cell type specific housekeeping genes ACTB (A, C), RPL32 (B) or CYC1 (D). n.d., not detected. Values are shown as means; error bars are shown as SD. Statistical significance was assessed by one-way ANOVA with multiple comparisons showing significant differences between Mock and infected cells (*$p \leq 0.05$, **$p<0.01$, ***$p<0.001$).

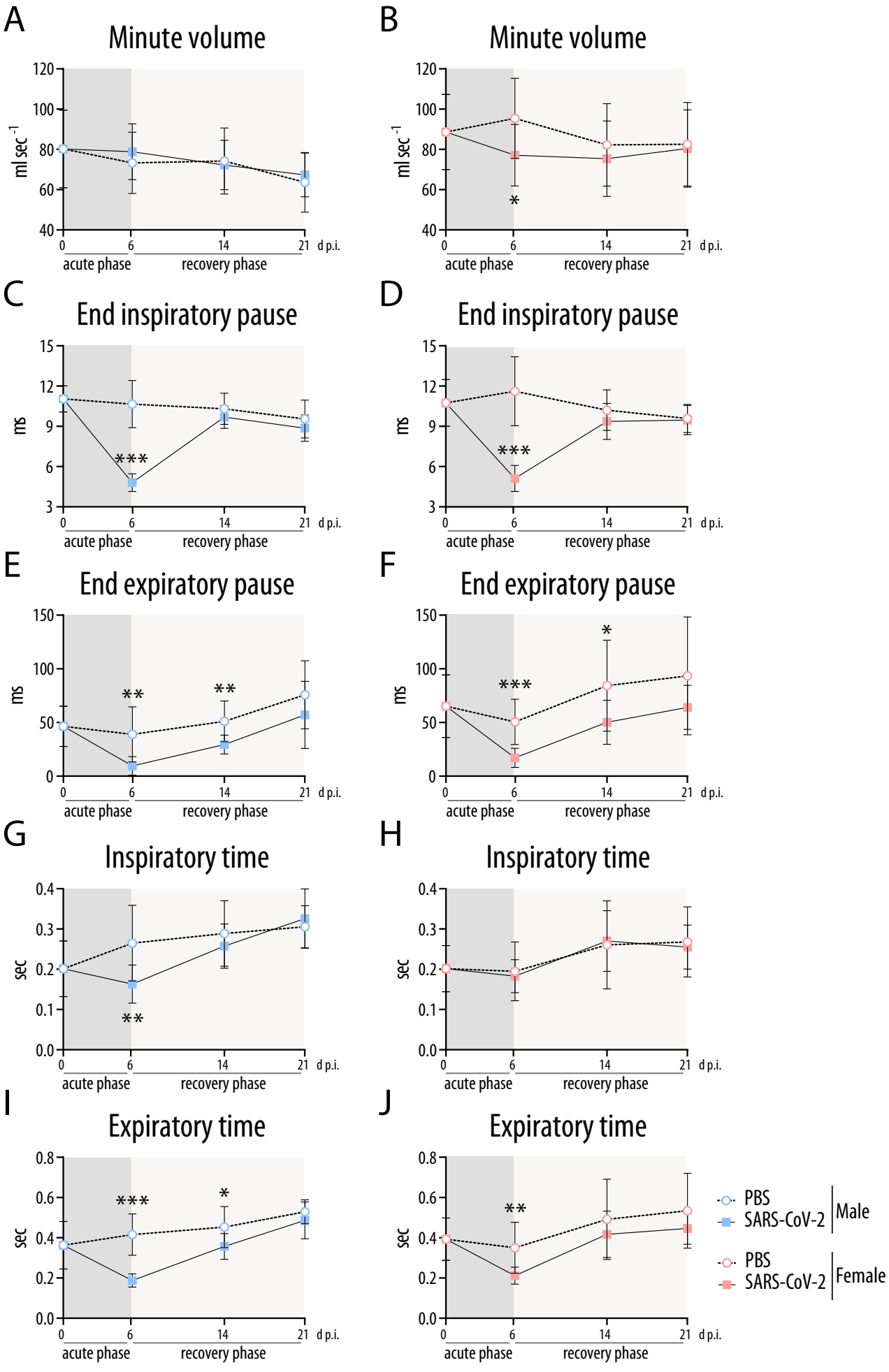
A
Minute volume
ml sec -1
120
100
80
60
40
0
6
14
21
d p.i.
acute phase
recovery phase
B
Minute volume
ml sec -1
*
C
End inspiratory pause
ms
15
12
9
6
3
***
D
End inspiratory pause
ms
***
E
End expiratory pause
ms
150
100
50
0
**
**
F
End expiratory pause
ms
***
*
G
Inspiratory time
sec
0.4
0.3
0.2
0.1
0.0
**
H
Inspiratory time
sec
I
Expiratory time
sec
0.8
0.6
0.4
0.2
0.0
***
*
J
Expiratory time
sec
**
PBS
SARS-CoV-2
Male
PBS
SARS-CoV-2
Female

Figure S6: Lung plethysmography in SARS-CoV-2 infected male and female golden hamsters, Related to Figure 5.

Whole-body plethysmography assessment of lung function parameters in SARS-CoV-2 infected or control (PBS) treated male (A, C, E, G, I) and female hamsters (B, D, F, H, J) at the indicated time points (n = 10; day 0 p.i. n = 12): Minute volume (A, B), end inspiratory pause (C, D), end expiratory pause (E, F), inspiratory time (G, H) and expiratory time (I, J). Values are shown as means; error bars are shown as SD. Statistical significance was assessed by unpaired Student´s t-test (*$p \leq 0.05$, **$p<0.01$, ***$p<0.001$).

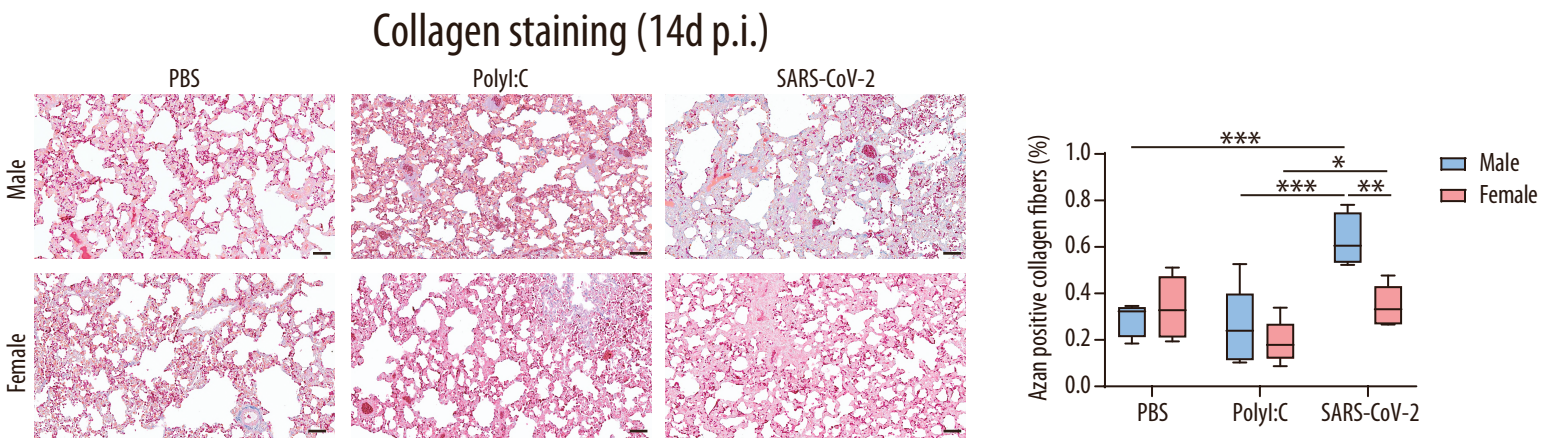

Figure S7. Lung histopathology of SARS-CoV-2 infected golden hamsters, Related to Figure 5.

Collagen staining with Azan of lung sections (left panel) and quantification thereof (right panel) from control (PBS) or SARS-CoV-2 infected male and female golden hamsters at day 14 p.i. (n = 4-5). Scale bar, 50 µm. Values are shown as means; error bars are shown as SD. Statistical significance was assessed by two-way ANOVA (*$p \leq 0.05$, **$p<0.01$, ***$p<0.001$).

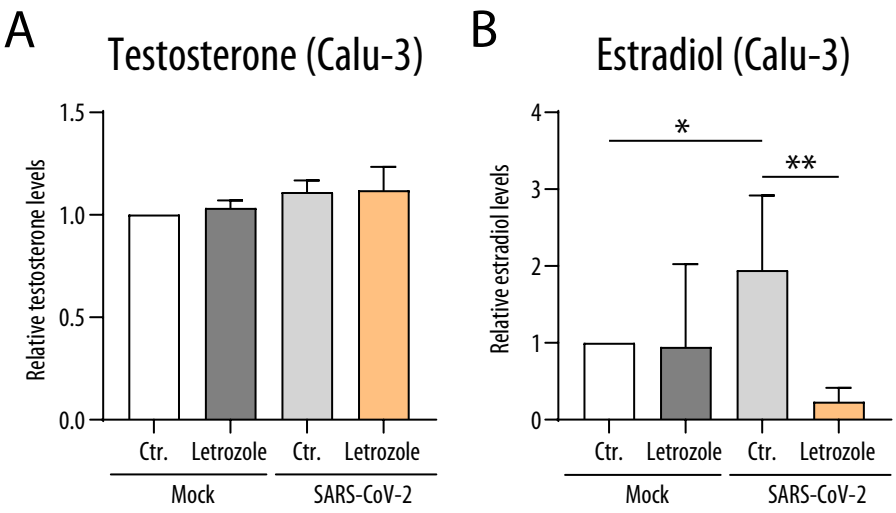

Figure S8. CYP19A1 activity in human lung cells upon SARS-CoV-2 infection, Related to Figure 6.

Testosterone (A) and estradiol (B) levels were measured in supernatants of Calu-3 cells either mock-infected (PBS) or infected with SARS-CoV-2 (MOI 0.01). After 24 h p.i., cells were treated with testosterone (100 nM) and the CYP19A1 inhibitor letrozole (1 μM) or as a control with DMSO (Ctr.). Samples were collected and analyzed 24 h post treatment. Shown is a merge of two to three independent biological replicates, each performed in technical triplicates. Values are shown as means; error bars are shown as SD. Statistical significance was assessed by unpaired Student's t-test (*$p \leq 0.05$, **$p<0.01$).

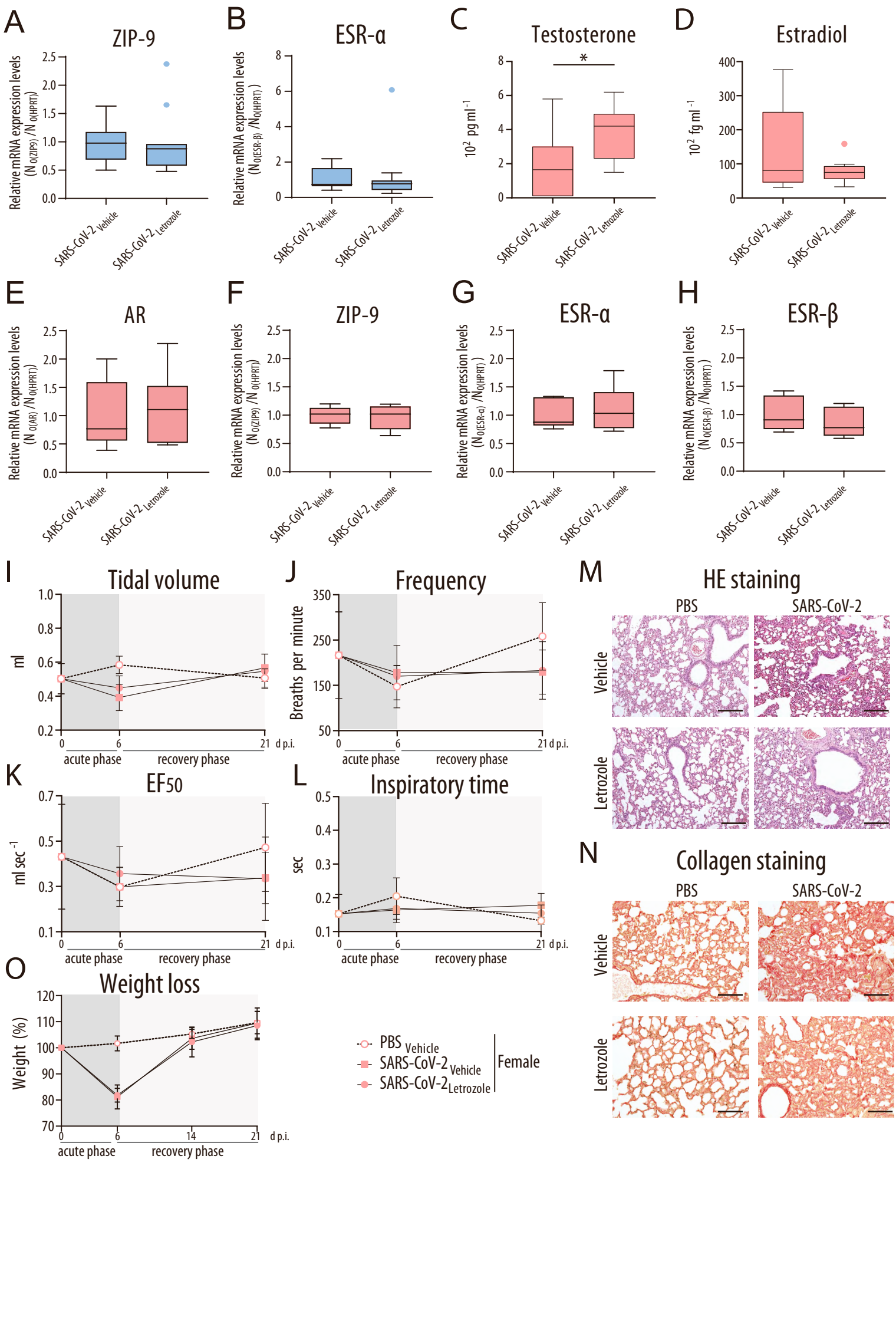
A
ZIP-9
Relative mRNA expression levels
B
ESR-α
C
Testosterone
D
Estradiol
E
AR
F
ZIP-9
G
ESR-α
H
ESR-β
SARS-CoV-2 Vehicle
SARS-CoV-2 Letrozole
I
Tidal volume
ml
J
Frequency
Breaths per minute
K
EF50
ml sec-1
L
Inspiratory time
sec
O
Weight loss
Weight (%)
acute phase
recovery phase
d p.i.
PBS Vehicle
SARS-CoV-2 Vehicle
SARS-CoV-2 Letrozole
Female
M
HE staining
PBS
SARS-CoV-2
Vehicle
Letrozole
N
Collagen staining

Figure S9. SARS-CoV-2 infected male and female hamsters treated with the CYP19A1 inhibitor letrozole, Related to Figure 6. (A, B) ZIP-9 (A) and ESR-α (B) mRNA expression levels measured in the lungs of SARS-CoV-2 infected male golden hamsters at day 6 p.i. (*n* = 11). SARS-CoV-2 infected and vehicle treated hamsters were set as 1. (C, D) Testosterone (C) and estradiol (D) levels were measured in SARS-CoV-2 infected female golden hamsters, treated either with vehicle or letrozole, at 3 d p.i. (*n* = 11). (E-H) AR (E), ZIP-9 (F), ESR-α (G) and ESR-β (H) mRNA expression levels measured in the lungs of SARS-CoV-2 infected female golden hamsters at day 6 p.i. (*n* = 6). SARS-CoV-2 infected and vehicle treated hamsters were set as 1 after normalization against HPRT. Data are shown as a box and whisker plot. (I-L) Whole-body plethysmography in control (PBS) or SARS-CoV-2 infected female golden hamsters, treated either with vehicle or letrozole: Tidal volume (I), frequency (J), EF50 (K) and inspiratory time (L) (*n* = 5-7; day 0 p.i. *n* = 12). (M, N) HE staining (M) or collagen staining with Sirius Red (N) of lung sections from control (PBS) or SARS-CoV-2 infected female golden hamsters, treated either with vehicle or letrozole, at 21 d p.i. Scale bar, 200 µm (M) or 100 µm (N) (*n* = 5-7 per group). (O) Weight loss of control (PBS) or SARS-CoV-2 infected female golden hamsters, treated either with vehicle or letrozole, over a time course of 21 days (*n* = 5-7 per group). (A-L, O) Values are shown as means; error bars are shown as SD. Statistical significance was assessed by Mann-Whitney test (*$p \leq 0.05$).

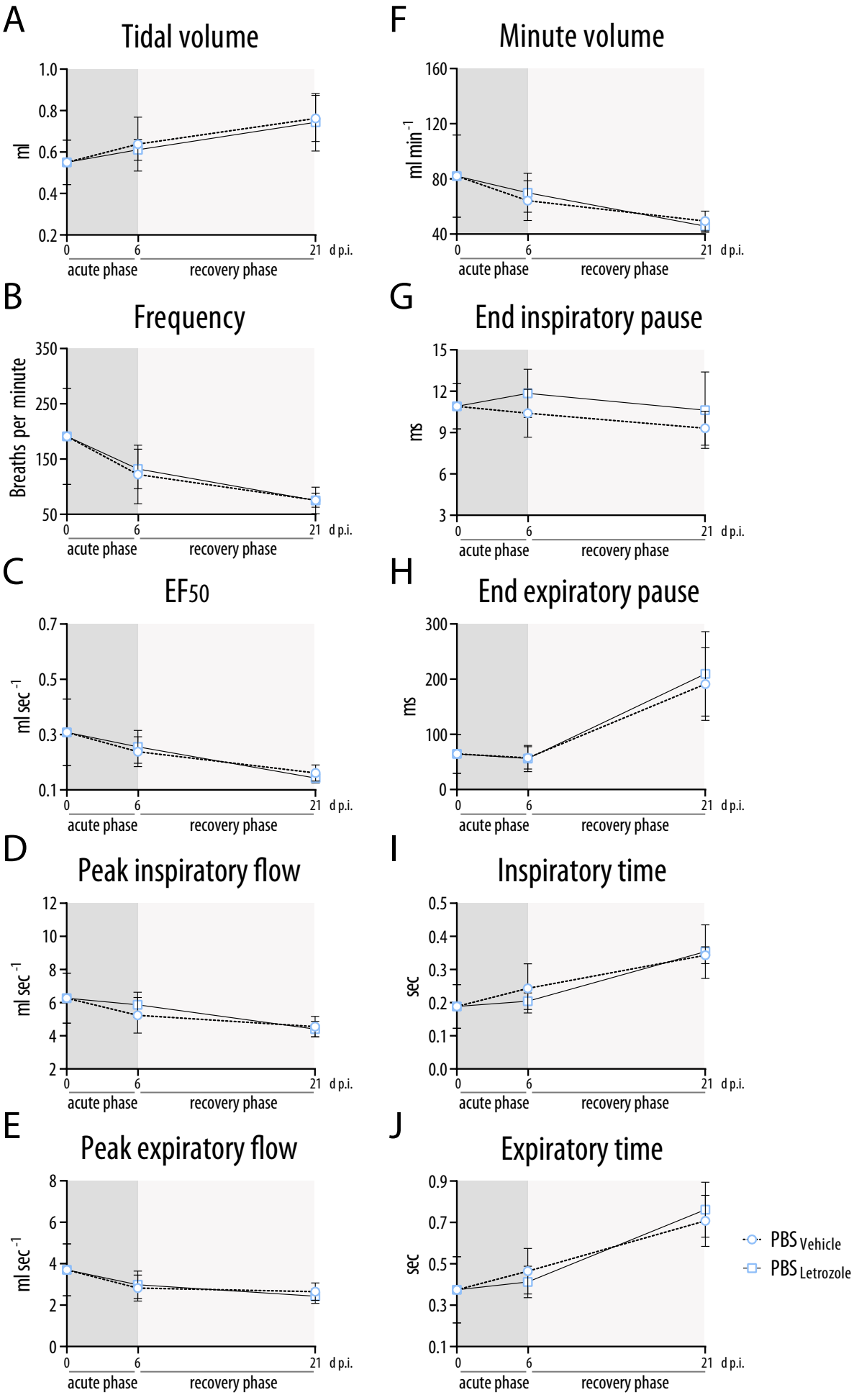
A
Tidal volume
ml
1.0
0.8
0.6
0.4
0.2
B
Frequency
Breaths per minute
350
250
150
50
C
EF50
ml sec-1
0.7
0.5
0.3
0.1
D
Peak inspiratory flow
ml sec-1
12
10
8
6
4
2
E
Peak expiratory flow
ml sec-1
8
6
4
2
0
F
Minute volume
ml min-1
160
120
80
40
G
End inspiratory pause
ms
15
12
9
6
3
H
End expiratory pause
ms
300
200
100
0
I
Inspiratory time
sec
0.5
0.4
0.3
0.2
0.1
0.0
J
Expiratory time
sec
0.9
0.7
0.5
0.3
0.1
0
6
21
d p.i.
acute phase
recovery phase
PBS Vehicle
PBS Letrozole

Figure S10. Lung plethysmography in PBS control infected male golden hamsters treated with the CYP19A1 inhibitor letrozole, Related to Figure 6.

Whole-body plethysmography assessment of lung function parameters in control (PBS) infected male hamsters, treated either with vehicle or letrozole, at the indicated time points (n = 5-7; day 0 p.i. n = 12): Tidal volume (A), frequency (B), EF50 (C), peak inspiratory flow (D), peak expiratory flow (E), minute volume (F), end inspiratory pause (G), end expiratory pause (H), inspiratory time (I) and expiratory time (J). Values are shown as means; error bars are shown as SD.

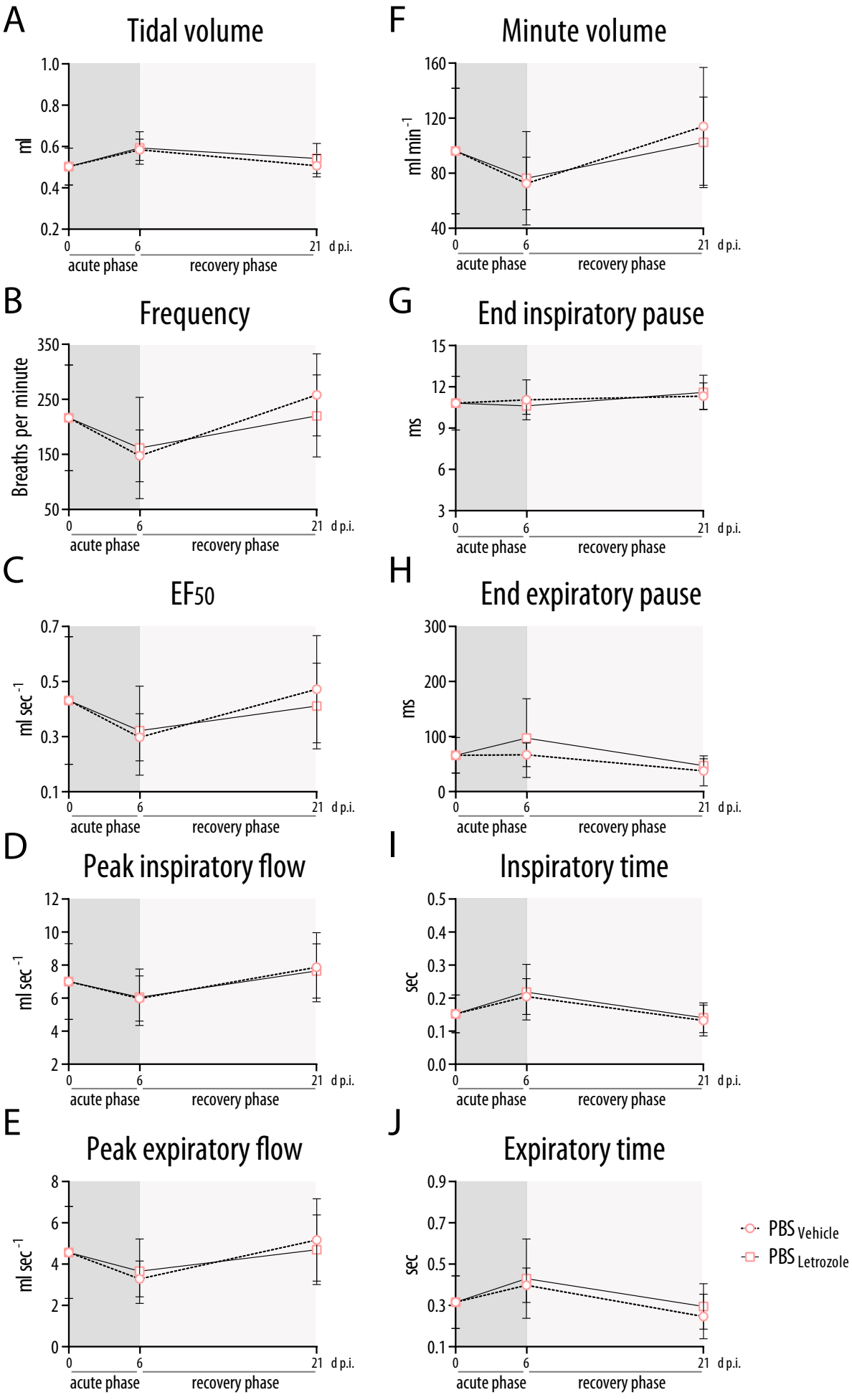
A
Tidal volume
ml
1.0
0.8
0.6
0.4
0.2
0
6
21
d p.i.
acute phase
recovery phase
F
Minute volume
ml min-1
160
120
80
40
B
Frequency
Breaths per minute
350
250
150
50
G
End inspiratory pause
ms
15
12
9
6
3
C
EF50
ml sec-1
0.7
0.5
0.3
0.1
H
End expiratory pause
ms
300
200
100
0
D
Peak inspiratory flow
ml sec-1
12
10
8
6
4
2
I
Inspiratory time
sec
0.5
0.4
0.3
0.2
0.1
0.0
E
Peak expiratory flow
ml sec-1
8
6
4
2
0
J
Expiratory time
sec
0.9
0.7
0.5
0.3
0.1
PBS Vehicle
PBS Letrozole

Figure S11. Lung plethysmography in PBS control infected female golden hamsters treated with the CYP19A1 inhibitor letrozole, Related to Figure 6.

Whole-body plethysmography assessment of lung function parameters in control (PBS) infected female hamsters, treated either with vehicle or letrozole, at the indicated time points (n = 5-7; day 0 p.i. n = 12): Tidal volume (A), frequency (B), EF50 (C), peak inspiratory flow (D), peak expiratory flow (E), minute volume (F), end inspiratory pause (G), end expiratory pause (H), inspiratory time (I) and expiratory time (J). Values are shown as means; error bars are shown as SD.

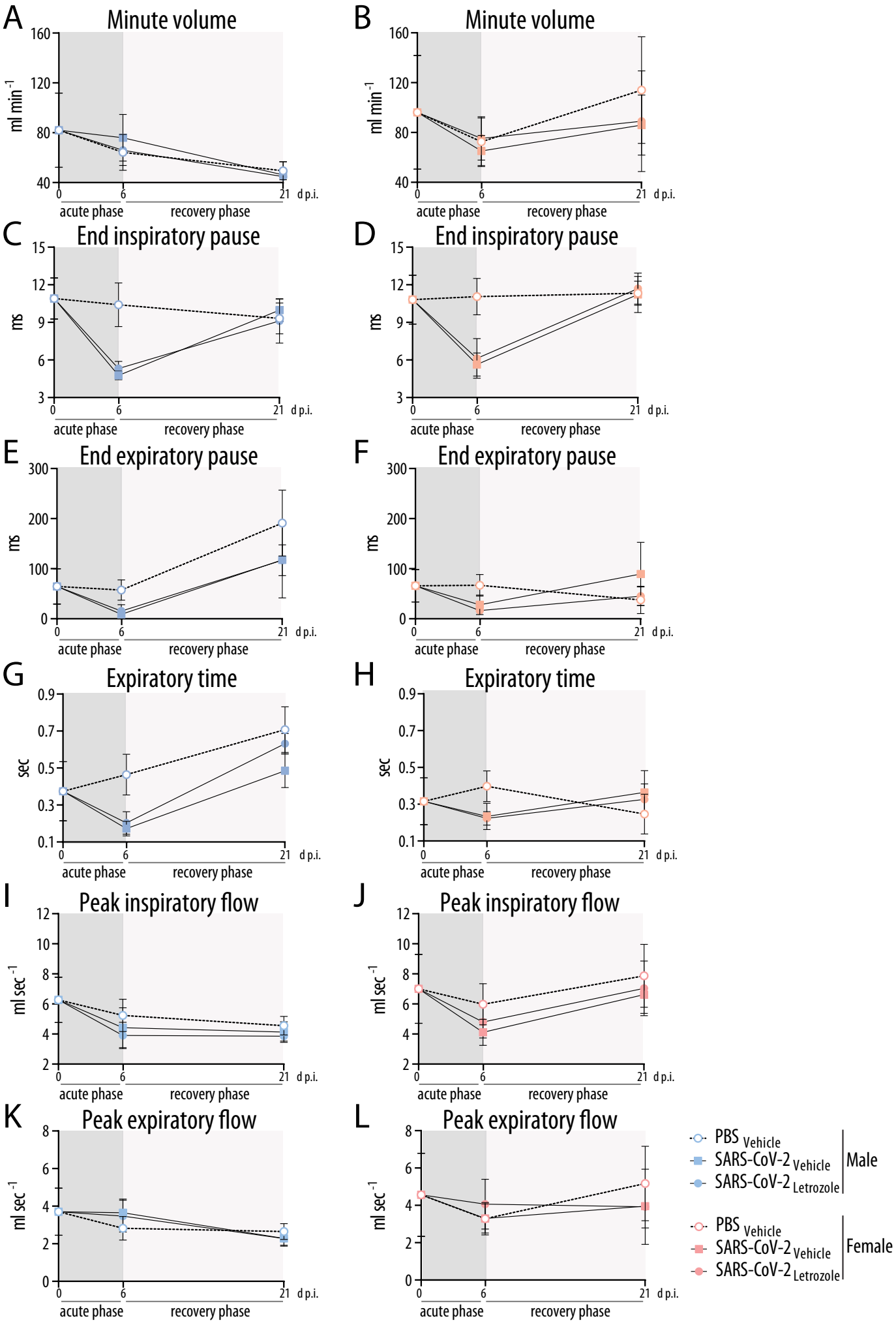
A
Minute volume
ml min-1
160
120
80
40
0
6
21
d p.i.
acute phase
recovery phase
B
Minute volume
C
End inspiratory pause
ms
15
12
9
6
3
D
End inspiratory pause
E
End expiratory pause
300
200
100
0
F
End expiratory pause
G
Expiratory time
sec
0.9
0.7
0.5
0.3
0.1
H
Expiratory time
I
Peak inspiratory flow
ml sec-1
12
10
8
6
4
2
J
Peak inspiratory flow
K
Peak expiratory flow
L
Peak expiratory flow
PBS Vehicle
SARS-CoV-2 Vehicle
SARS-CoV-2 Letrozole
Male
PBS Vehicle
SARS-CoV-2 Vehicle
SARS-CoV-2 Letrozole
Female

Figure S12. Lung plethysmography in SARS-CoV-2 infected male and female golden hamsters treated with the CYP19A1 inhibitor letrozole, Related to Figure 6.

Whole-body plethysmography assessment of lung function parameters in SARS-CoV-2 infected or control (PBS) infected male (A, C, E, G, I, K) and female hamsters (B, D, F, H, J, L), treated either with vehicle or letrozole, at the indicated time points (n = 5-7; day 0 p.i. n = 12): Minute volume (A, B), end inspiratory pause (C, D), end expiratory pause (E, F), expiratory time (G, H), peak inspiratory flow (I, J) and peak expiratory flow (K, L). Values are shown as means; error bars are shown as SD.

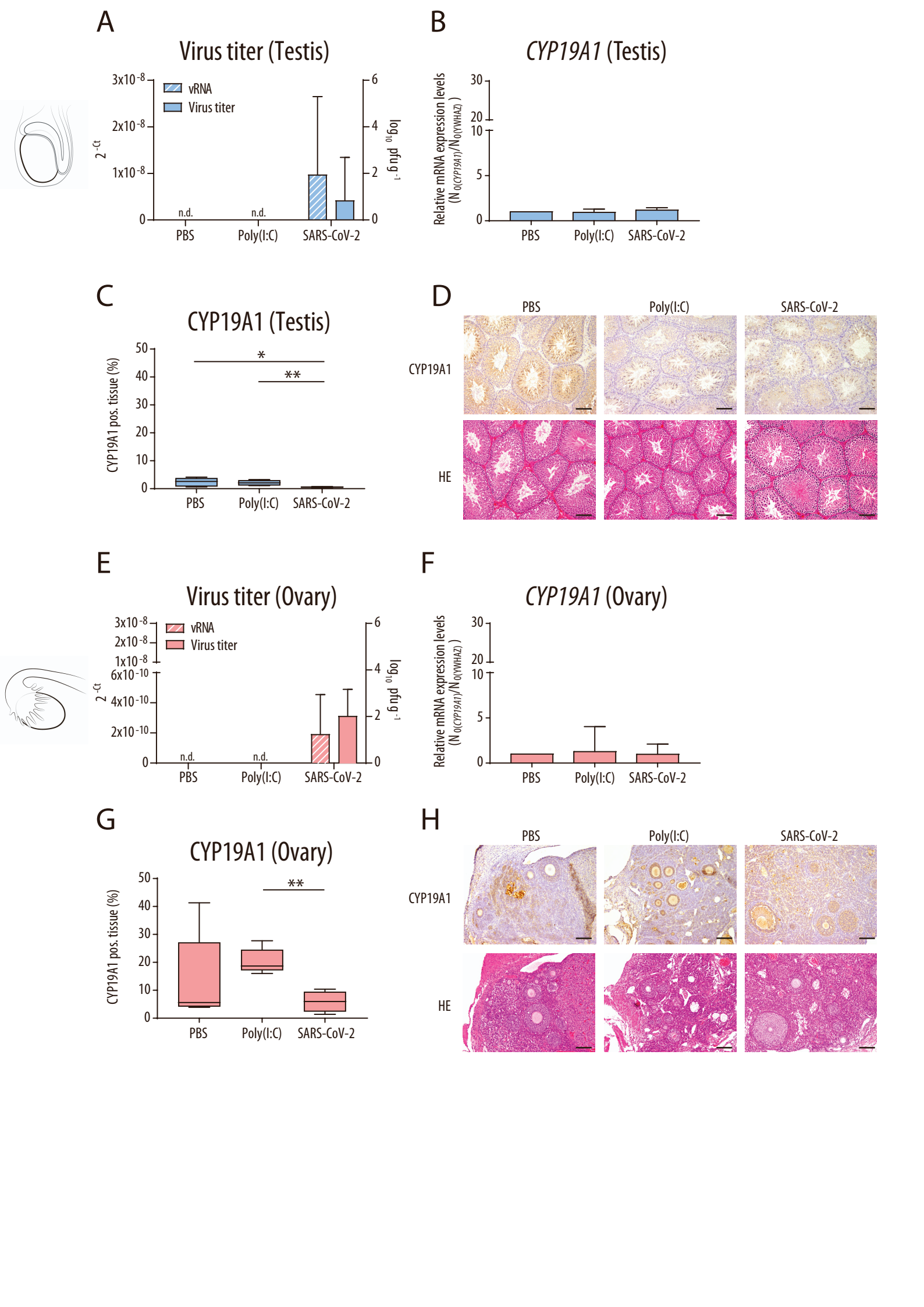
A
Virus titer (Testis)
vRNA
Virus titer
2-Ct
log10 pfu g-1
n.d.
n.d.
PBS
Poly(I:C)
SARS-CoV-2
B
CYP19A1 (Testis)
Relative mRNA expression levels
C
CYP19A1 (Testis)
CYP19A1 pos. tissue (%)
*
**
D
CYP19A1
HE
E
Virus titer (Ovary)
F
CYP19A1 (Ovary)
G
CYP19A1 (Ovary)
H

Figure S13. Virus titer and CYP19A1 expression in the gonads of SARS-CoV-2 infected male and female golden hamsters, Related to Figure 3.

(A, E) Viral mRNA and virus titer detected in the testis of SARS-CoV-2 infected and control treated (PBS, Poly(I:C)) male (A) and ovaries of female (E) golden hamsters at day 3 d p.i. (n = 5). n.d., not detectable. (B, F) CYP19A1 mRNA expression levels measured in the testis of SARS-CoV-2 infected and control treated (PBS, Poly(I:C)) male (B) and ovaries of female (F) golden hamsters at day 3 p.i. (n = 5). Relative CYP19A1 mRNA expression values in PBS treated hamsters were set to 1 after normalization against YWHAZ. (C, G) Quantification of CYP19A1 protein expressing tissue in the testis of SARS-CoV-2 infected and control treated (PBS, Poly(I:C)) male (C) and ovaries of female (G) golden hamsters at day 3 p.i. (n = 5). (D, H) CYP19A1 protein expression detected by immunohistochemistry in the testis of SARS-CoV-2 infected and control treated (PBS, Poly(I:C)) male (D) and ovaries of female (H) golden hamsters. Consecutive slides were also stained with HE. Representative pictures of each group are shown (n = 5). Scale bar, 100 µm. (A, B, E, F) Values are shown as means; error bars are shown as SD. (C,G) Values are shown as a box and whisker plot. Statistical significance was assessed by one-way ANOVA (*$p \leq 0.05$, **$p<0.01$).

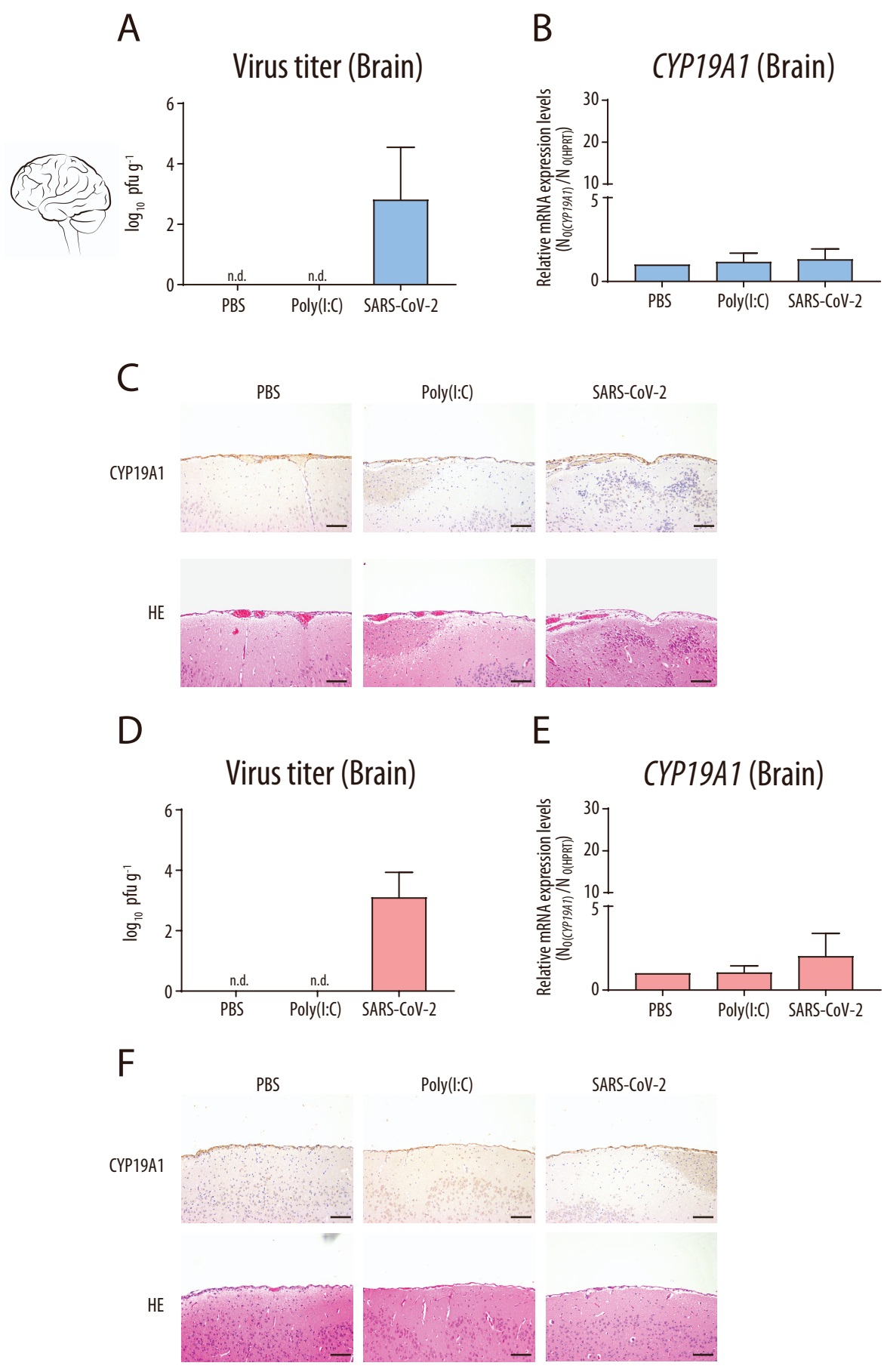
A
Virus titer (Brain)
log10 pfu g-1
6
4
2
0
n.d.
n.d.
PBS
Poly(I:C)
SARS-CoV-2
B
CYP19A1 (Brain)
Relative mRNA expression levels
(N0(CYP19A1)/N0(HPRT))
30
20
10
5
0
PBS
Poly(I:C)
SARS-CoV-2
C
PBS
Poly(I:C)
SARS-CoV-2
CYP19A1
HE
D
Virus titer (Brain)
log10 pfu g-1
6
4
2
0
n.d.
n.d.
PBS
Poly(I:C)
SARS-CoV-2
E
CYP19A1 (Brain)
Relative mRNA expression levels
(N0(CYP19A1)/N0(HPRT))
30
20
10
5
0
PBS
Poly(I:C)
SARS-CoV-2
F
PBS
Poly(I:C)
SARS-CoV-2
CYP19A1
HE

Figure S14. Virus titer and CYP19A1 expression in the brains of SARS-CoV-2 infected male and female golden hamsters, Related to Figure 3.

(A, D) Virus titer detected in the brains of SARS-CoV-2 infected and control treated (PBS, Poly(I:C)) male (A) and female (D) golden hamsters at day 3 p.i. (*n* = 5). n.d., not detectable. (B, E) CYP19A1 mRNA expression levels measured in the brains of SARS-CoV-2 infected and control treated (PBS, Poly(I:C)) male (B) and female (E) golden hamsters at day 3 p.i. (*n* = 5). Relative CYP19A1 mRNA expression values in PBS treated hamsters were set to 1 after normalization against HPRT. (C, F) CYP19A1 protein expression detected by immunohistochemistry in the brains of SARS-CoV-2 infected and control treated (PBS, Poly(I:C)) male (C) and female (F) golden hamsters. Consecutive slides were also stained with HE. Representative pictures of each group are shown (*n* = 5). Scale bar, 100 μm. (A, B, D, E) Values are shown as means; error bars are shown as SD.

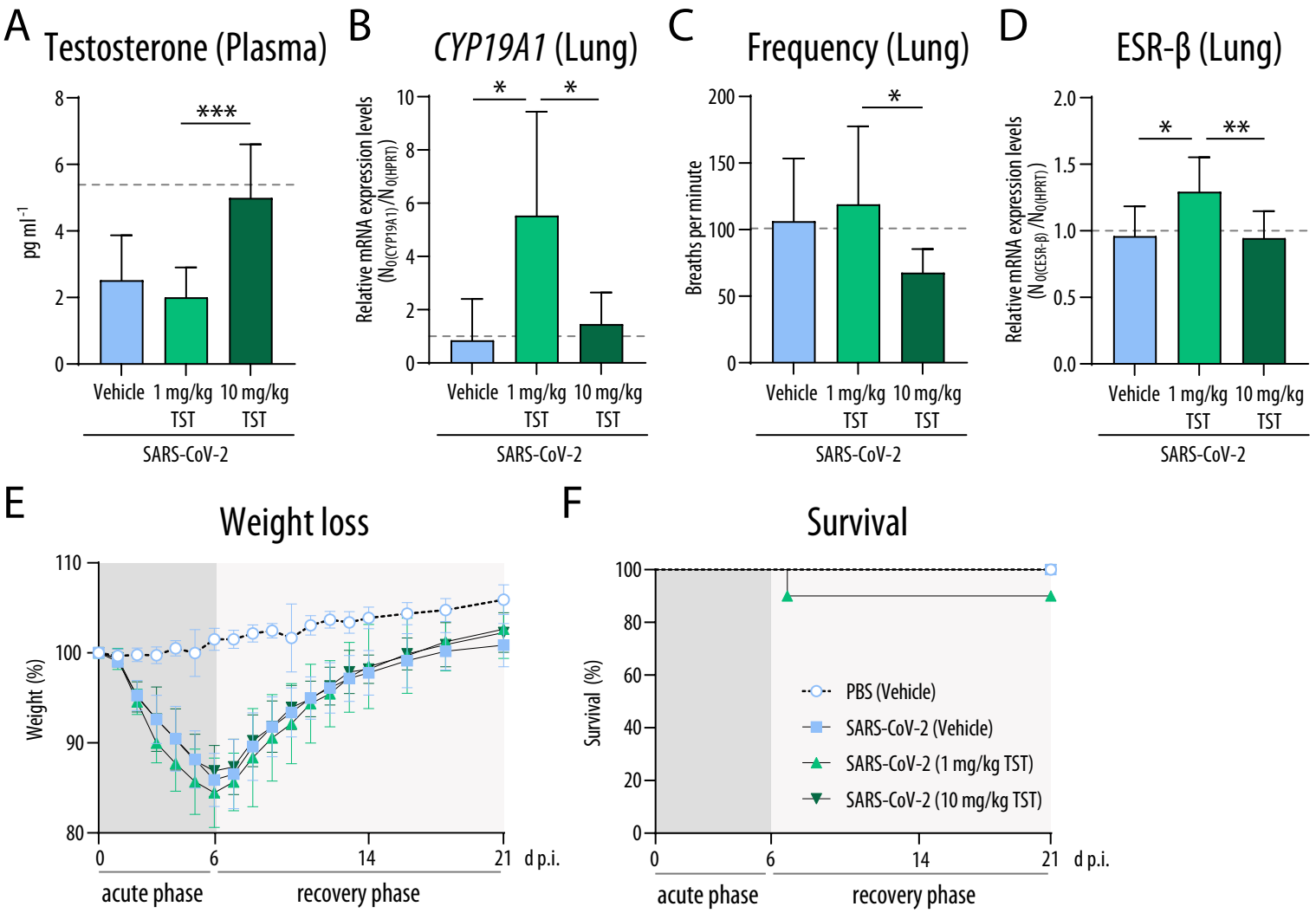

Figure S15. Effect of testosterone treatment on CYP19A1 expression and SARS-CoV-2 pathogenesis in male golden hamsters, Related to Figures 3, 4 and 5.

Male golden hamsters were infected with SARS-CoV-2 and either treated with vehicle, 1mg/kg or 10 mg/kg testosterone (TST). As control, male golden hamsters were inoculated with PBS and treated with vehicle (grey dash line). (A-D) Testosterone levels (A), CYP19A1 mRNA expression levels in the lungs (B), frequency as a lung function parameter measured by whole-body plethysmography (C) and ESR-β mRNA expression levels in the lungs (D) were determined in all groups at day 21 p.i. (n = 10; SARS-CoV-2 treated with 1 mg/kg TST: n = 9). (B, D) Relative CYP19A1 and ESR-β mRNA expression values in PBS and vehicle treated hamsters were set to 1 after normalization against HPRT. (E, F) weight loss (E) and survival (F) of control treated as well as SARS-CoV-2 infected and TST treated male golden hamsters over a time course of 21 days (n = 10 per group). Values are shown as means; error bars are shown as SD. Statistical significance was assessed by unpaired Student´s t-test (*p ≤ 0.05, **p<0.01, ***p<0.001).

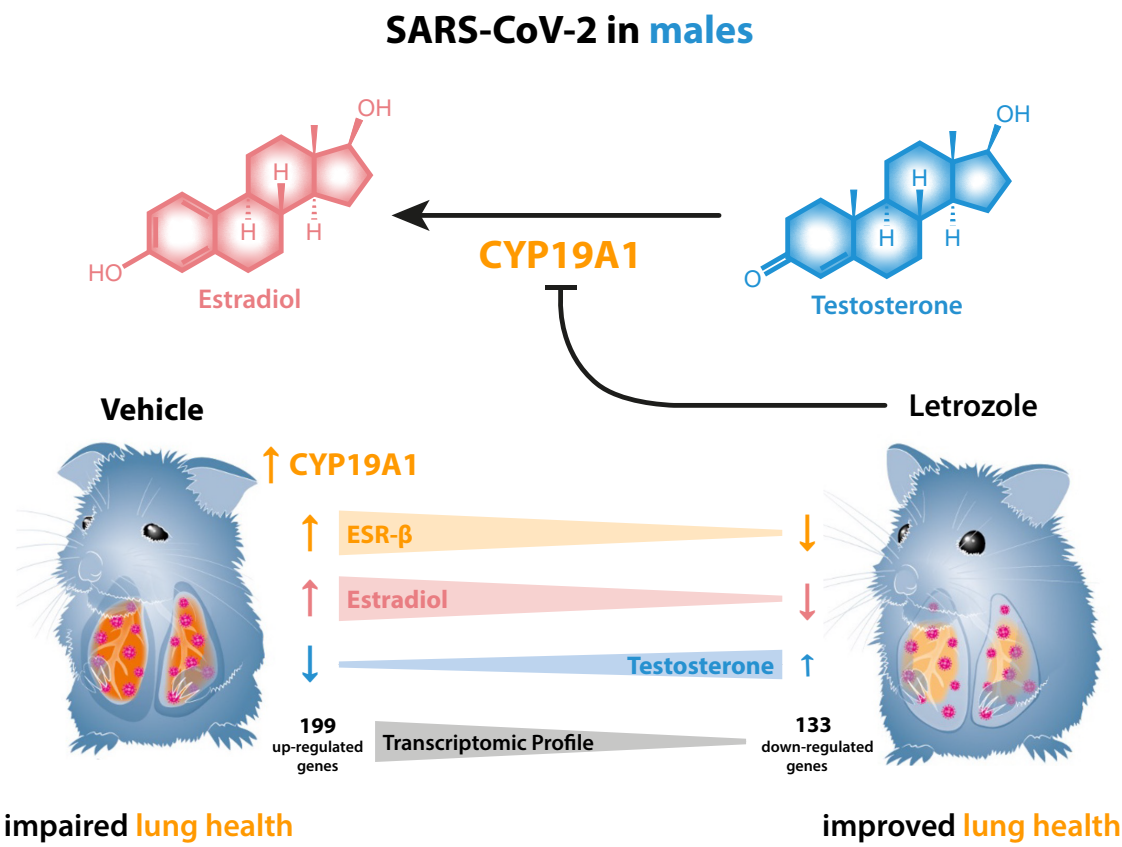

Figure S16. Summary Model: Letrozole mediated improved lung health in SARS-CoV-2 infected males, Related to Figure 6. Treatment of hamsters with the CYP19A1 inhibitor letrozole results in reduced estradiol and ESR-ß levels, while testosterone levels are elevated. Letrozole treatment results in the downregulation of 133 genes in SARS-CoV-2 infected males, as compared to the SARS-CoV-2 infected, vehicle-treated control group. In summary, reduced estradiol levels, reduced ESR-ß expression and elevated testosterone levels are associated with improved overall lung health in SARS-CoV-2 infected, letrozole-treated male hamsters.